

Production of two Higgses at the Large Hadron Collider in CP-violating MSSM

Priyotosh Bandyopadhyay^{a,1} and Katri Huitu^{a,2}

^a*Department of Physics, and Helsinki Institute of Physics,
P.O.Box 64 (Gustaf H  llstr  min katu 2), FIN-00014 University of Helsinki, Finland*
Email: ¹priyotosh.bandyopadhyay@helsinki.fi, ²katri.huitu@helsinki.fi

ABSTRACT: Production of two Higgs bosons is studied in a CP violating supersymmetric scenario at the Large Hadron Collider with $E_{cm} = 14$ TeV. There exists a region where a very light Higgs $\lesssim 50$ GeV could not be probed by LEP experiment. This leads to so called 'LEP hole' region. Recently LHC found a Higgs boson around ~ 125 GeV, which severely constrains the possibility of having lighter Higgs bosons, which cannot be detected, i.e., buried Higgs, in this model. We investigate the possibility of buried Higgs bosons along with the direct and indirect bounds coming from LEP, LHC and other experiments. In particular we take into account the constraints from EDM and from B -observables. We analyse first the case where a Higgs boson mass is around 125 GeV and the other two Higgs masses are below 100 GeV and not observabed so far. In the second case the lightest Higgs boson mass is around 125 GeV and the other two are decoupled. We analyse the production of two Higgses and their decay modes leading to various final states for these benchmark points. We perform a collider simulation with PYTHIA and Fastjet where we consider all the major backgrounds. Among the final states we have analysed, we find that $2b + 2\tau$ is promising and the signal significance is 5σ at an integrated luminosity $\lesssim 10 \text{ fb}^{-1}$. For some benchmark points it is also possible to observe the light Higgs mass peak. We also explore the leptonic final state which could be instrumental in the precision measurement of a very light Higgs.

KEYWORDS: Higgs, CP-violation, Supersymmetry, LHC.

Contents

1. Introduction	1
2. CP violating scenario and the experimental constraints	3
3. Benchmark points for collider study	4
4. Collider phenomenology	6
4.1 Sig1: $3b + 2\tau$	10
4.2 Sig2: $2b + 2\tau$	13
4.3 Sig3: 2ℓ	13
5. Summary and discussion	14

1. Introduction

CP violation is among the phenomena which are not fully understood in the context of the Standard Model (SM). Although CP violation exists in the SM, and agrees well with the laboratory experiments, there is an inconsistency between the amount of violation and matter content of the Universe, and it is argued that new sources of CP violation are needed.

Many of the proposals for beyond the SM (BSM) physics do contain new sources for CP violation. In this work we consider Minimal Supersymmetric Standard Model (MSSM). It has been shown in the literature that the tree-level CP invariance of the MSSM Higgs potential can be violated by loop effects involving CP-violating interactions of Higgs bosons to top and bottom squarks [1, 2, 3, 4, 5, 6]. In such a scenario with explicit CP-violation at tree-level, the neutral Higgses (h_i , $i=1,2,3$) mix the CP states at loop-level. It has been shown that [2, 4, 5] loop-induced CP-violation modifies the tree-level Higgs coupling such that light Higgs in this scenario could be $\lesssim 60$ GeV and can escape the detection at LEP2.

For example, it has been shown that assuming universality of gaugino masses (M_i , $i=1,2,3$) at some high scale and assuming corrections from third generation strong sector, the CP-violating MSSM Higgs sector can be parametrised in terms of a few independent phases [7]: the phase of Higgsino mass parameter (also called μ term), i.e., $\text{Arg}(\mu)$, and the phase of soft trilinear supersymmetry (SUSY) breaking parameters, i.e., $\text{Arg}(A_f)$, with $f = t, b$. The experimental upper bounds on the electric dipole moments (EDMs) of electrons and neutrons [8, 9] as well as of mercury atoms [10] constrain these phases.

Before Large Hadron Collider (LHC) found out a Higgs resonance with mass around 125 GeV [11, 12, 13, 14] earlier colliders had given bounds on the Higgs mass. For the SM

Higgs boson, mass bound from the LEP collider is $m_h > 114.4$ GeV [15, 16], and Tevatron excludes Higgs for the mass ranges $m_h \sim 147 - 180$ GeV and $100 - 103$ GeV but finds an excess in 115-135 GeV region [17]. In the MSSM with real and CP-conserving parameters, the experimental lower limit on the lightest Higgs boson is ~ 90 GeV [18] for any $\tan\beta$. The lower bound on the mass of the lightest Higgs boson of the CP-conserving MSSM from LEP [16] can be drastically reduced or may even entirely vanish if non-zero CP-violating phases are allowed [19, 20]. This can happen through radiative corrections to the Higgs potential, whereby the above mentioned phases of the μ parameter and the A parameters enter into the picture [1, 21].

With the discovery of ~ 125 GeV Higgs at the LHC the question of a buried Higgs remains to be answered. The LHC experiment will look in all possible different decay modes to find an extra scalar which would be lighter than 100 GeV. Finding of such scalar(s) will be certainly a proof of BSM Higgs but also the possibility of CP-violating MSSM will come into the picture. The phenomenology of such a light Higgs has been studied in the context of CPV-MSSM in a benchmark scenario known as 'CPX' [1, 21].

In the CPX scenario the ZZh_1 coupling can be strongly reduced because of the CP violating phases, and the LEP mass limit for the lightest Higgs boson can be lowered to 50 GeV or even less, depending on $\tan\beta$. Thus the LEP searches leave a hole in $(m_{h_1}, \tan\beta)$ parameter space [16]. Complementary channels such as $e^+e^- \rightarrow h_1h_2$ suffer also phase space suppression within the hole region. At Tevatron, this CP violation and the Higgs phenomenology has been studied [22, 23].

Within the hole region in addition to ZZh_1 coupling, $WW h_1$ and tth_1 are suppressed and thus the lightest Higgs boson h_1 is difficult to discover. In the context of CPX scenarios there has been quite a few studies performed in the SM production channels [24] as well as in the supersymmetric channels [25, 26, 27]. In the context of CP-conserving MSSM, cascade Higgs production has been studied in [28].

Most of these earlier studies do not fit with the data for ~ 125 GeV Higgs and the other experimental constraints coming from EDMs and the rare B -decays. In this article we consider the recent SUSY mass bounds from LHC along with the Higgs results. We take into account thallium EDM result and constraints coming from $\text{Br}(B_s \rightarrow s\gamma)$ and $\text{Br}(B_s \rightarrow \mu\mu)$. We look for the possibility of the buried Higgs or the decoupled Higgs scenarios as two possibilities. In this context we study the Higgs pair production. We consider the $H \rightarrow b\bar{b}, \tau\bar{\tau}, \ell\bar{\ell}$ decay modes for possible final states. We find that $2b + 2\tau$ channel is very promising in searching for a very light Higgs ($m_{h_1} \sim 30$ GeV) and $\lesssim 10 \text{ fb}^{-1}$ of integrated luminosity will be enough to have 5σ significance over the dominant SM backgrounds. For the precision measurement leptonic channel would be crucial. We also find out that Higgs productions in association with Z will also contribute to these final states. One can differentiate between the two types of contributions by constructing the heavier Higgs mass peak, i.e., $m_{h_{2,3}}$ in the corresponding channels at very high luminosity.

We will also point out that in certain benchmark points the two Higgs production through coupling of three Higgs bosons is important, and thus we have a possibility to probe the Higgs potential at those points. Obviously construction of the Higgs potential would be of fundamental importance.

The paper is organised as follows. In Section 2 we review the CPX benchmark scenario and discuss the experimental constraints. We also discuss very briefly the possibilities of evading such bounds. In section 3 we define the benchmark points consistent with the experimental results for the collider study. The corresponding production cross-section and the decay branching fractions are listed in this section. In section 4 we carry out collider simulation for 14 TeV LHC for the desired final states. Finally in section 5 we summarise.

2. CP violating scenario and the experimental constraints

It is known [1, 21] that the CP -mixing term in the Higgs sector is generated at quantum level and proportional to $Im(\mu A_t)/M_{SUSY}^2$. The well known CPX scenario predicts that certain parameters are related:

$$\begin{aligned} m_{\tilde{t}} &= m_{\tilde{b}} = m_{\tilde{\tau}} = M_{SUSY}, \quad |A_t| = |A_b| = |A_{\tau}| = 2M_{SUSY}, \\ arg(A_t) &= arg(A_b) = arg(A_{\tau}) = 90^\circ. \end{aligned} \quad (2.1)$$

In particular the parameter space with $M_{SUSY} = 500$ GeV is of special phenomenological interest along with the other parameters that are compatible with the LEP “hole” and are given below,

$$\begin{aligned} M_{SUSY} &= 500 \text{ GeV}, \quad |m_{\tilde{g}}| = 1 \text{ TeV}, \quad M_2 = 2M_1 = 200 \text{ GeV}, \\ arg(A_{b,\tau}) &= 90^\circ, \quad arg(m_{\tilde{g}}) = 90^\circ, \quad \tan \beta = 5 - 10. \end{aligned} \quad (2.2)$$

In addition, $\tan \beta$ and m_{H^\pm} are the free input parameters that could be varied to achieve various points in the ‘LEP hole’. The consequences of the CPX scenario have been studied in [29].

Recently new results from LHC have changed the scenario as most of the parameter region is ruled out. In this paper we shall take into account the Higgs discovery around ~ 125 GeV which has been reported by the CMS and ATLAS collaborations [11, 12]. Along with the recent LHC Higgs results we also consider the Higgs bounds from LEP [30]. We can see that buried Higgs, i.e., a very light Higgs ($\lesssim 60$ GeV), is still possible in MSSM. The possibility of a light Higgs could be an artifact of explicit CP-violation in the Lagrangian and then a loop-induced CP-violation in the Higgs sector as explained in the introduction.

The recent studies on some indirect variables show that they can constrain these CP-violating phases and eventually can rule out a large amount of parameter space. The bounds on the CP-violating MSSM coming from various dipole-moment measurements have been studied in details [31]. In this paper we consider the constraints coming from electric-dipole moment (EDM) of thallium with the current 2σ upper bound $|d_{Tl}| < 1.3 \times 10^{-24}$ e cm [33]. For this purpose we vary the relative angles between M_1 , M_2 and also ϕ_{A_t} , ϕ_{M_3} ; where we denote $Arg(A_f) = \phi_f$ and $Arg(M_i) = \phi_{M_i}$. In this region the one loop-SUSY contribution and light Higgs mediated two-loop contribution are comparable and tend to

cancel each other. Thus it is possible to achieve the desired EDM bounds. Here we would like to mention that a very light Higgs ($m_{h_1} \lesssim 8$ GeV) is ruled out from bottomonium decay $\Upsilon(1S) \rightarrow \gamma h_1$ [34].

We also look into the flavour constraints coming from the B -observables. For this purpose we first consider $\text{Br}(B_s \rightarrow \mu\mu)$, which recently has come down by two orders of magnitude [35] can severely constrain this scenario. $\text{Br}(B_s \rightarrow \mu\mu)$ grows large as $\tan\beta$ increases. For the cancellation we use GIM operative point mechanism [36]: we vary $\rho = \frac{Q_{1,2}}{Q_3}$, the ratio of first two generation of the squark masses over the third generation squark masses. The cancellation happens when $\rho \sim 0.8 - 1.9$. This predicts very light first two generation masses for some cases. To evade such light mass bound coming from $\text{jets} + \cancel{p}_T$ at the LHC [37], LSP mass must be large which would make the jets rather soft.

Next we consider the bounds coming from $\text{Br}(B_s \rightarrow X_s \gamma)$ [38]. Unlike $B_s \rightarrow \mu\mu$ case $\text{Br}(B_s \rightarrow X_s \gamma)$ decreases as $\tan\beta$ increases. This is because the charged Higgs contribution is suppressed due to the threshold corrections at large $\tan\beta$ [39]. We also included recent bounds on third-generation squark masses and on LSP from 8 TeV LHC [40]. To have light third-generation mass (M_{SUSY}), the LSP needs to be relatively heavy, i.e., around 300 GeV [40]. We also choose $m_3 = 1.4$ TeV to satisfy recent gluino mass bound [37, 41]. For this choice of gluino mass we find that it is very difficult to get $m_{h_3} \gtrsim 124$ GeV by using CPsuperH [42]¹. We vary $\tan\beta$ and m_{H^\pm} as usual as we move to different points in the 'LEP hole'. The Higgs mass spectrum depends on the radiative correction which is very sensitive to top mass. The central value of m_t has shifted frequently during the years. These shifts change the size of the hole, although the location remains almost the same. We use for the top mass 173.2 ± 0.9 GeV as referred by Tevatron [44].

3. Benchmark points for collider study

After above investigation we find three points in explicit CP-violating MSSM which are no longer so called "CPX" points but experimentally allowed ones. Allowed regions of the parameter space have very different but attractive phenomenological consequences. Table 1 describes the benchmark points that we consider for our collider study. We consider three different scenarios:

1. Two light Higgses are buried and have masses < 100 GeV and mass of the heaviest one is around 125 GeV.
2. The lightest Higgs is very light $m_{h_1} \leq 30$ GeV, so that $h_3 \rightarrow h_1 Z$ is allowed. The second lightest is also buried, $m_{h_2} \leq 100$ GeV and mass of the third one 125 GeV as in the previous case.
3. This is a decoupled scenario where the heavier Higgses are decoupled with masses ≥ 500 GeV and the lightest one has $m_{h_1} \sim 125$ GeV.

¹There is $\sim 2 - 3$ GeV uncertainty in Higgs mass calculated by CPsuperH and FeynHiggs [43]. For this paper we have used CPsuperH2.0 for the mass spectrum and the other observables.

Parameters	BP1	BP2	BP3
$\tan \beta$	30	30	20
m_{H^\pm}	115	115	500
μ	1400	2000	1000
M_1	300	300	300
ϕ_{M_1}	66	66	40
M_2	400	400	400
ϕ_{M_2}	0	0	0
M_3	1400	1400	1400
ϕ_{M_3}	61	61	60
A_t	1000	1000	1000
ϕ_{A_t}	60	60	60
A_b	11200	4200	1000
ϕ_{A_b}	35	35	90
A_τ	14200	16100	1000
ϕ_{A_τ}	90	90	90
ρ	0.83	0.88	1.90
m_{h_1}	54.25	25.00	123.50
m_{h_2}	95.00	94.70	490.70
m_{h_3}	124.40	124.60	494.70

Table 1: Input parameters in the benchmark points within the ‘LEP-hole’ and the corresponding CP-violating neutral Higgs masses. The angles are given in the unit of degree and other parameters are in GeV except $\tan \beta$ which is unitless.

Benchmark Points	Cross-section in fb					
	$\sigma_{h_1 h_2}$	$\sigma_{h_1 h_3}$	$\sigma_{h_1 h_1}$	$\sigma_{h_2 h_2}$	$\sigma_{h_3 h_3}$	$\sigma_{h_2 h_3}$
BP1	908.02	47.02	5393.50	24.11	7.83	6.92
BP2	1858.89	45.23	33086.7	20.35	5.19	3.91
BP3	1.73×10^{-2}	1.0×10^{-2}	18.6	8.6×10^{-3}	5.7×10^{-3}	0.47

Table 2: Cross-sections (in fb) of two Higgs productions ($h_{2,3}h_i = 1, 2, 3$) at the LHC with $E_{cm} = 14$ TeV for the benchmark points.

In this study, we focus on two Higgs production processes, i.e., $h_i h_j$, $i=1,2,3$ and $j=2,3$. We investigate the various possible decays of the Higgs bosons which will lead to the corresponding final states. We also include Higgs production in association with a Z boson. Table 2 presents the cross-sections of two Higgs boson productions ($h_i h_j, i, j = 1, 2, 3$) for the three benchmark points at the LHC with $E_{cm}=14$ TeV and Table 3 presents the cross-sections of Higgs boson productions associated with a Z boson for the center of mass energy of 14 TeV.

Table 4 and Table 5 present the decay branching fractions of h_1 , h_2 and h_3 , respectively.

Benchmark Points	Cross-section in fb		
	$\sigma_{h_1 Z}$	$\sigma_{h_2 Z}$	$\sigma_{h_3 Z}$
BP1	513.18	155.39	672.74
BP2	1180.31	150.248	672.93
BP3	708.56	59.00	53.86

Table 3: Cross-sections (in fb) of Higgs productions ($h_{2,3}h_i = 1, 2, 3$) associated with Z boson at the LHC with $E_{cm} = 14$ TeV for the benchmark points.

Benchmark points	h_1 decays			
	$b\bar{b}$	$\tau\bar{\tau}$	WW	ZZ
BP1	0.70	0.29	-	-
BP2	0.67	0.32	-	-
BP3	0.67	0.076	0.14	0.017

Table 4: The dominant branching fractions of the lightest Higgs boson h_1 for the benchmark points.

From Table 4 we can see that for all the three benchmark points the lightest Higgs, h_1 mostly decays to $\tau\tau$ and $b\bar{b}$. In case of BP3, we have two additional decay modes WW and ZZ . Similar to h_1 , we can see from Table 5 that h_2 also mainly decays to $\tau\tau$ and $b\bar{b}$. There is also a possibility to decay into $h_1 Z$, the branching fractions of which are rather small. In case of BP2 and BP3 $h_2 \rightarrow h_1 h_1$ has small but non-zero branching fraction. Table 5 shows that the heaviest neutral Higgs h_3 mainly decays to h_1 pair for BP1 and BP2. In case of BP3 it decays to τ and b pairs like h_1 .

4. Collider phenomenology

In this study, **CalcHEP** [45] is used to calculate the cross-sections, the decay branching fractions and also to generate the events. The couplings and mass spectra are originally generated from the program **CPsuperH2.2** [42] which is used by **CalcHEP** via calling the program **CPsuperH2.2**. The standard **CalcHEP**-**PYTHIA** interface [46], which uses the **SLHA** interface [47] was then used to pass the **CalcHEP**-generated events to **PYTHIA** [48]. Furthermore, all relevant decay information is generated with **CalcHEP** and is passed to **PYTHIA** through the same interface. All these are required since there is no public implementation of CP violating MSSM in **PYTHIA**. Subsequent decays of the produced particles, hadronization and the collider analyses are done with **PYTHIA (version 6.4.5)**.

We use **CTEQ6L** parton distribution function (PDF) [49, 50]. In **CalcHEP** we opted for the lowest order α_s evaluation, which is appropriate for a lowest order PDF like **CTEQ6L**.

Branching fraction								
Benchmark	h_2 decays				h_3 decays			
points	$b\bar{b}$	$\tau\bar{\tau}$	$h_1 Z$	$h_1 h_1$	$b\bar{b}$	$\tau\bar{\tau}$	$h_1 Z$	$h_1 h_1$
BP1	0.68	0.316	1.0×10^{-4}	-	0.01	8.7×10^{-3}	1.6×10^{-5}	0.98
BP2	0.62	0.36	1.0×10^{-3}	0.01	6.7×10^{-3}	8.2×10^{-3}	3.4×10^{-4}	0.98
BP3	0.79	0.19	3.1×10^{-4}	1.4×10^{-3}	0.79	0.19	1.2×10^{-4}	1.9×10^{-3}

Table 5: The dominant branching fractions of heavier Higgs bosons(h_2 and h_3) for the benchmark points.

The renormalization/factorization scale in **CalcHEP** is set at $\sqrt{\hat{s}}$. This choice of scale results in a somewhat conservative estimate for the event rates.

For hadronic level simulation we have used **Fastjet-3.0.3** [51] algorithm for the jet formation with the following criteria:

- the calorimeter coverage is $|\eta| < 4.5$
- $p_{T,min}^{jet} = 20$ GeV and jets are ordered in p_T
- leptons ($\ell = e, \mu$) are selected with $p_T \geq 20$ GeV and $|\eta| \leq 2.5$
- no jet should match with a hard lepton in the event
- $\Delta R_{lj} \geq 0.4$ and $\Delta R_{ll} \geq 0.2$
- Since efficient identification of the leptons is crucial for our study, we required, on top of the above set of cuts, that hadronic activity within a cone of $\Delta R = 0.3$ between two isolated leptons should be $\leq 0.5 p_T^\ell$ GeV in the specified cone.

In the CP-violating scenario, h_1 decays dominantly into $b\bar{b}$ and $\tau\bar{\tau}$ (see Table 4) for all the benchmark points as discussed in the earlier section. In cases of BP1 and BP2 where the light Higgs h_1 is relatively light (< 60 GeV), b -quarks lead to soft jets and the b -tagging efficiency is small. To illustrate this, we present in Figure 1 the ordered p_T distributions for b -jets coming from $h_1 h_3$ for BP1 and from $h_1 h_1$ for BP3. We see that for BP1, the lowest p_T b -jet can be very soft, $p_T \leq 40$ GeV. For this analysis we have required a b -jet tagging efficiency ($\geq 50\%$) [52].

Next we study the jet-multiplicity distribution for $h_1 h_3$ for BP1, BP2 and the dominant background $t\bar{t}$. We can see from Figure 2 that the two Higgs production has fewer jets than the $t\bar{t}$. Demanding $n_{jets} \leq 4$ removes most of the $t\bar{t}$ background events. Thus it could be a very useful tool to kill the SM background as well as the SUSY cascade backgrounds which usually have a large number of jets.

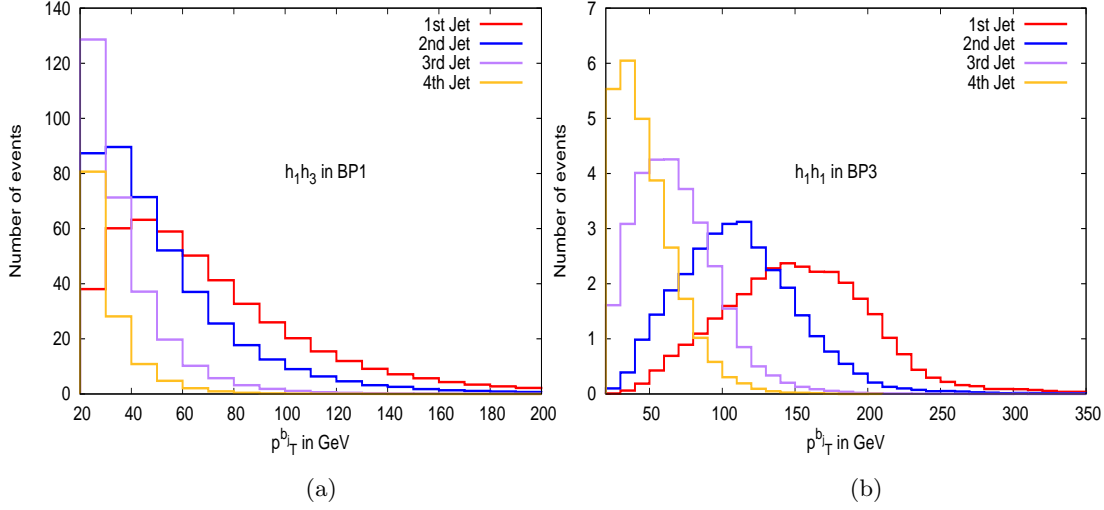


Figure 1: p_T^{bjet} distribution for h_1h_3 (a) for BP1 and for h_1h_1 (b) for BP3 at an integrated luminosity of $\mathcal{L} = 10 \text{ fb}^{-1}$.

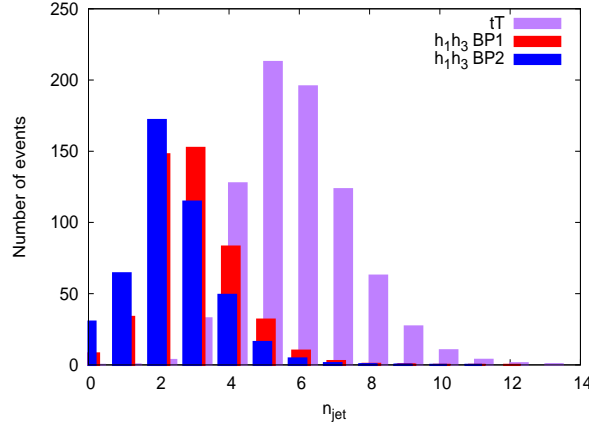


Figure 2: Jet multiplicity distributions for h_1h_3 for BP1, BP2 and $t\bar{t}$ at an integrated luminosity of $\mathcal{L} = 10 \text{ fb}^{-1}$.

To see the status of the b -final states we first check the b -jet invariant mass. Figure 3 shows the invariant mass of two b -jets which satisfy the above mentioned criteria at an integrated luminosity of 10 fb^{-1} at the LHC with center of mass energy of 14 TeV . In Figure 3(a) the b -jet invariant mass comes from h_1h_1 signal for the three benchmark points. The lightest Higgs boson peaks are visible for all three benchmark points. In Figure 3(b) we show both the lightest Higgs h_1 peak as well as the second lightest Higgs peak h_2 , which come from h_1h_2 for BP1 and BP2². Similarly Figure 3(c) describe the b -jet pair invariant mass distribution for BP1 and BP2 coming from h_1h_3 signal. Due to small cross-section the mass resolutions are not clear unlike the other two production channels.

²For BP3 the number of events are not enough to plot the b -jet pair invariant mass distribution

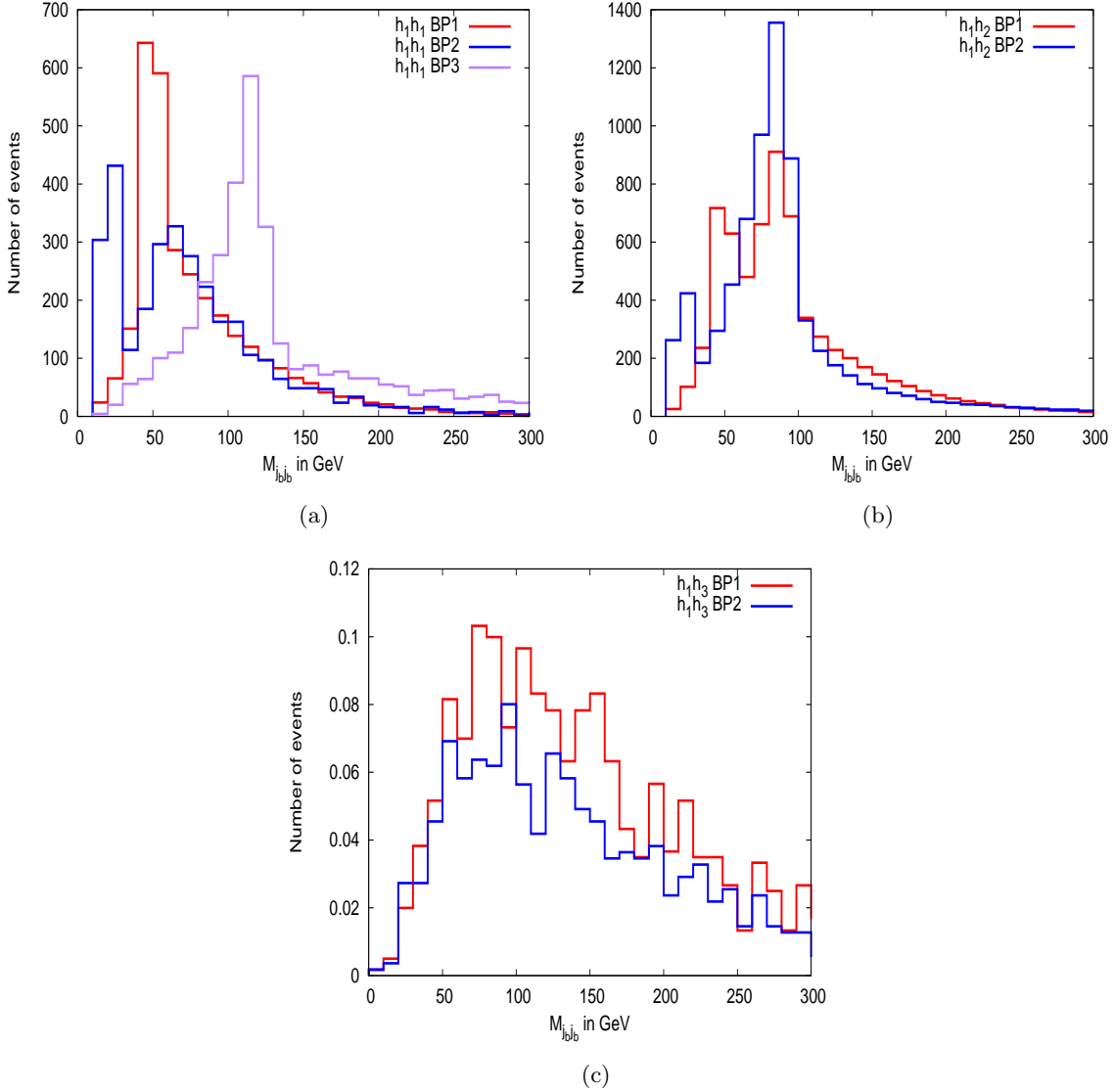


Figure 3: b -jet invariant mass distribution coming (a) from $h_1 h_1$, (b) from $h_1 h_2$ and (c) from $h_1 h_3$ for benchmark points at an integrated luminosity of $\mathcal{L} = 10 \text{ fb}^{-1}$.

All three Higgs bosons decay to τ pairs with branching fraction $\sim 8 - 30\%$ except for h_3 whose branching fraction to τ pairs is $\mathcal{O}(10^{-3})$ for BP1 and BP2 (see Table 4 and Table 5). For a very light Higgs, in cases of BP1 and BP2, the taus coming from h_1 can be very soft. Boost of the light Higgs (h_1) of course increases the p_T of taus. Figure 4(a) shows the p_T distribution of the partonic τ coming from $h_1 h_1$ production channel. We can clearly see τ s coming from h_1 decay for BP1 and BP2 will have enough boost to tag them as tau-jet. Figure 4(b) shows that in case of $h_1 h_3$ production channel the boost of τ s increases further.

Taus coming from Higgs then decay to pions through one prong or/and three prong decay. In the present study, we use the one-prong (one charged track) hadronic decays

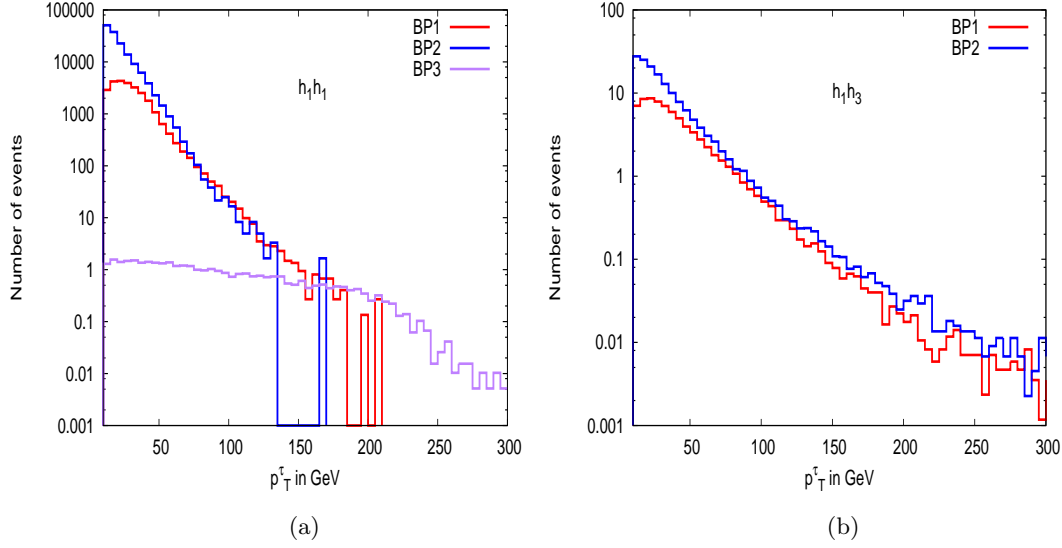


Figure 4: p_T distribution of partonic τ coming from h_1h_1 and h_1h_3 for the benchmark points at an integrated luminosity of $\mathcal{L} = 10 \text{ fb}^{-1}$. Due to small production cross-section of h_1h_3 for BP3, the generated events are not enough for the distribution.

of the τ -leptons which have a collective branching fraction of about 50% of which almost 90% is comprised of final states with π^\pm , ρ and a_1 mesons. To establish a jet as a τ -jet we take the following approach. We first check, for each jet coming out of **Fastjet** within $|\eta| \leq 2.5$, if there is a partonic τ within a cone of $\Delta R \leq 0.4$ about the jet-axis. If there is one, then we further ensure that there is a single charged track within a cone of $\Delta R \leq 0.1$ of the same jet axis. This marks a narrow jet character of a τ -jet. Of course there is an efficiency associated to such kind of a geometric requirement which is a function of p_T of the concerned jet and has been demonstrated in the literature [53, 54].

Next we study the τ final state by plotting the hadronic τ -jet invariant mass. In Figure 5 we plot the invariant mass distribution of two hadronic τ -jets coming from the Higgs boson decay. In Figure 5(a) the contribution comes from h_1h_1 production as before and it is easily seen that the lightest Higgs mass peaks are much clearer than the b -jet invariant mass distributions. Figure 5(b)& (c) show the contribution coming from the production of h_1h_2 and h_1h_3 , respectively for BP1 and BP2. In case of Figure 5(c) the h_3 mass peak is not visible as h_3 mostly decays to h_1 pair for both BP1 and BP2 (see table 5).

So far we have seen that the final states with b and τ -jets could be prompted for all the benchmark points if we consider the production channels, i.e., $h_ih_j, i, j = 1, 2, 3$. Let us first discuss the final states with b and τ .

4.1 Sig1: $3b + 2\tau$

The final state $3b + 2\tau$ is possible when at least one Higgs is heavy, i.e., h_2 or h_3 , which decays to $Z h_1$ or h_1h_1 . If at least one lightest Higgs h_1 decays to tau lepton pair and the other h_1 or Z decays to b pairs then we have $4b + 2\tau$ final state. This scenarios is possible

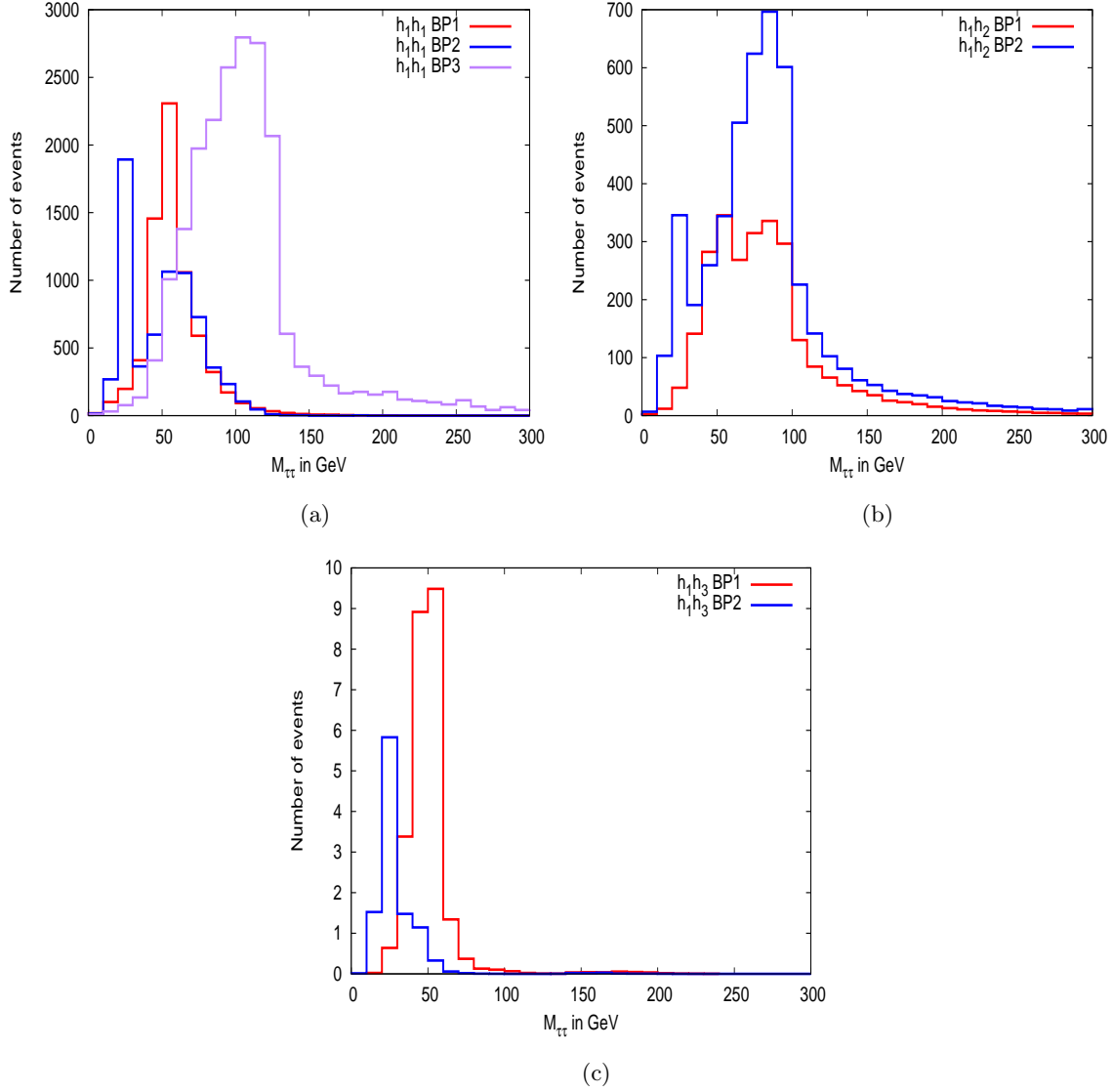


Figure 5: τ -jet invariant mass distribution coming (a) from h_1h_1 , (b) from h_1h_2 and (c) from h_1h_3 for benchmark points at an integrated luminosity of $\mathcal{L} = 10 \text{ fb}^{-1}$.

for BP1 and BP2:

$$\begin{aligned}
pp &\rightarrow h_1h_{2,3}, \\
&\rightarrow h_1Zh_1(\text{or } h_1h_1) \rightarrow 4b + 2\tau.
\end{aligned}
\tag{4.1}$$

The b -tagging efficiency is around 50%, so tagging 4 b -jets will bring down the number of signal events. This is the reason we study the $3b + 2\tau$ final state. We choose the final state as:

$$\text{sig1} : n_{\text{jets}} \leq 5 + (\geq 3b - \text{jet}) + (\geq 2\tau - \text{jet}) + (p_T \leq 30 \text{ GeV}).$$

We consider $t\bar{t}$, $t\bar{t}Z$, $t\bar{t}W$, ZZ and $t\bar{t}b\bar{b}$ as the main SM backgrounds. Table 6 presents the number of events for sig1 for signal and backgrounds at an integrated luminosity of 10 fb^{-1} . Table 6 also presents the numbers of events with window cut of $\pm 10 \text{ GeV}$ around the mass peak of respective invariant mass distribution. Here we give the number of events with the window cuts around h_1 , h_2 and h_3 for both $b\bar{b}$ and $\tau\tau$ invariant mass distribution. Determination of these mass peaks depends on the relative number of signal events over background events.

Signal	Benchmark Points			Backgrounds				
	BP1	BP2	BP3	$t\bar{t}$	$t\bar{t}Z$	$t\bar{t}W$	ZZ	$t\bar{t}b\bar{b}$
sig1	52.30	21.60	0.80	1.00	0.00	0.00	0.80	0.06
sig1+ $ m_{b\bar{b}} - m_{h_1} \leq 10 \text{ GeV}$	25.30	8.80	0.20	0.00	0.00	0.00	0.00	0.00
sig1+ $ m_{b\bar{b}} - m_{h_2} \leq 10 \text{ GeV}$	3.70	2.10	0.00	0.10	0.00	0.00	0.00	0.00
sig1+ $ m_{b\bar{b}} - m_{h_3} \leq 10 \text{ GeV}$	1.80	0.12	0.00	0.00	0.00	0.00	0.00	0.00
sig1+ $ m_{\tau\tau} - m_{h_1} \leq 10 \text{ GeV}$	33.70	19.00	0.09	0.00	0.00	0.00	0.00	0.00
sig1+ $ m_{\tau\tau} - m_{h_2} \leq 10 \text{ GeV}$	33.70	19.00	0.09	0.00	0.00	0.00	0.60	0.00
sig1+ $ m_{\tau\tau} - m_{h_3} \leq 10 \text{ GeV}$	0.07	0.20	0.00	0.00	0.00	0.00	0.00	0.00

Table 6: Number of events after the selection cuts for sig1 final states for the benchmark points and backgrounds at an integrated luminosity of 10 fb^{-1} at the LHC with $E_{cm} = 14 \text{ TeV}$.

From Table 6 we see that Sig1 has 7.1σ significance over background for BP1 at an integrated luminosity of 10 fb^{-1} . For BP2 and BP3 it is 4.5σ and 0.5σ , respectively. For h_1 peak we can get $\geq 5\sigma$ significance for BP1 for both $b\bar{b}$ and $\tau\tau$ invariant mass distribution. The corresponding numbers for BP2 are 3σ and 4.4σ respectively. In case of h_2 and h_3 peak, for a comparable signal significance over background one needs to go for higher luminosity.

Next we consider the case when two of the h_1 decay to tau pairs and the final state is $(\geq 2b - jet) + (\geq 4\tau - jet)$. The decay branching fraction of $h_1 \rightarrow \tau\tau$ is around 30% which is much lower than the $h_1 \rightarrow b\bar{b}$ branching fraction. The tau coming from such a light Higgs (h_1) is of low p_T which reduces the τ detection efficiency. Because of these two effects the final state does not have many events at 10 fb^{-1} integrated luminosity.

There is a possibility that the heavier Higgses ($h_{2,3}$) decay to $h_1 Z$ in the case of $h_1 h_{2,3}$ productions, which leads to $h_1 h_1 Z$. Similarly $h_{2,3} Z$ production also leads to the above final state when $h_{2,3} \rightarrow h_1 h_1$. When Z decays to lepton pair and if we tag only $3b$ then it can give final state like $3b + OSD + (|m_{\ell\ell} - M_Z| \leq 5 \text{ GeV}) + (p_T \leq 30 \text{ GeV})$, where OSD corresponds to opposite sign dilepton.

Comparing the production cross-sections from Table 2 and decay branching fractions from Table 4 and Table 5, we see that the contribution from $h_1 h_{2,3}$ production would be negligible due to low $h_{2,3} \rightarrow h_1 Z$ branching fraction for the chosen benchmark points. On the other hand $h_3 Z$ has relatively large production cross section at least for BP1 and BP2 but fails to contribute due to demand of $3b$ tagging coming from very light Higgs (h_1). One needs to go for very high luminosity to look for this final state.

4.2 Sig2: $2b + 2\tau$

Unlike for the other benchmark points, in BP3, $h_3 \rightarrow h_1 h_1$ is very small, and h_3 mostly decays to b or tau pairs. Thus the final state with $2b + 2\tau$ looks promising. Thus both the heavy($h_{2,3}$) and light (h_1) Higgs bosons can decay either to b pair or τ pair which leads to $2b + 2\tau$ final state. If the bs and τs are coming from the heavier Higgs ($h_{2,3}$), then they have a high p_T . On the other hand when they come from the light Higgs (h_1) they have a very low p_T . We study the final state as:

$$\text{sig2 : } n_{\text{jets}} \leq 5 + (\geq 2b - \text{jet}) + (\geq 2\tau - \text{jet}) + (p_T \leq 30 \text{ GeV}).$$

Table 7 presents the number of events for the signal and backgrounds at an integrated luminosity of 10 fb^{-1} . We can see that sig2 has 13.5σ , 10σ and 0.6σ significance with 10 fb^{-1} of luminosity for BP1, BP2 and BP3, respectively. This could be a useful channel to look for the light Higgs scenarios. We then put a window cut in the $b\bar{b}$ invariant mass distribution around the light Higgs mass peak (m_{h_1}) as $|m_{b\bar{b}} - m_{h_1}| \leq 10 \text{ GeV}$. The signal significance for this case does not change much from the previous one and it is 12σ and 10.4σ for BP1 and BP2. The buried Higgs scenarios can be probed at the LHC. Even when we put the window cut around the next mass peak, i.e., $|m_{b\bar{b}} - m_{h_2}| \leq 10 \text{ GeV}$, the signal significance for BP1 and BP2 still remains around 5σ at an integrated luminosity of 10 fb^{-1} . For heavier Higgs mass peak resolution, i.e for m_{h_3} one needs to go to higher luminosity, at least to 43 fb^{-1} of luminosity in the case of BP1 and BP2. We also investigate the scenario where we take window cuts around $\tau\tau$ invariant mass peak. In this case the reach for the Higgs mass peaks is possible in relatively higher luminosity.

4.3 Sig3: 2ℓ

In this section we will see the exclusive leptonic final states, i.e., the final states with μ and e . Though the branching fractions of Higgses to lepton pair are very small, these tiny branching fractions can be crucial for precision measurement of invariant mass peak. The leptonic channel is particularly handy when it comes to determination of a very small Higgs mass ($\lesssim 50 \text{ GeV}$). In Figure 6 the lepton p_T distribution comes from (a) $h_1 h_3$ for BP1 and (b) $h_1 h_1$ for BP3. Clearly leptons for BP1 can be treated as hard leptons ($p_T \geq 20 \text{ GeV}$) but for BP3 they can be as hard as 200 GeV .

Figure 7 describes the dilepton invariant mass coming (a) from $h_1 h_1$ and (b) from $h_1 h_2$. From Figure 7(a) we can see the h_1 peaks for all three benchmark points. On the other hand Figure 7(b) shows both the Higgs mass peaks, i.e., h_1 around 30 and 50 GeV , h_2 around 95 GeV .

We first analyse the dilepton final states which could be interesting in determining the very light Higgs scenario with precision. We define the final state as: sig3 : 2ℓ . Table 8 presents the number of events for the final state sig3 for both signal and backgrounds at an integrated luminosity of 10 fb^{-1} . The dominant background events are coming from $t\bar{t}$ and gauge boson pair production (VV). The signal significance for the dilepton final state (sig3) reaches 5σ for BP2 only. The signal significance for BP1 crosses 3σ at 10 fb^{-1} of luminosity. For the light Higgs (h_1) mass peak the significance is 7.6σ for BP2 at 10 fb^{-1}

Signal	Benchmark Points			Backgrounds				
	BP1	BP2	BP3	$t\bar{t}$	$t\bar{t}Z$	$t\bar{t}W$	ZZ	$t\bar{t}b\bar{b}$
sig2	501.30	350.80	19.00	812.10	0.30	0.50	57.70	0.20
sig2+ $ m_{bb} - m_{h_1} \leq 10$ GeV	195.00	129.00	4.00	65.00	0.04	0.05	6.20	0.00
				23.70	0.00	0.00	0.60	0.00
				59.00	0.05	0.05	0.60	0.00
sig2+ $ m_{bb} - m_{h_2} \leq 10$ GeV	69.00	56.00	0.00	103.00	0.01	0.08	15.00	0.06
				104.10	0.01	0.08	16.00	0.06
				1.0	0.00	0.00	0.00	0.00
sig2+ $ m_{bb} - m_{h_3} \leq 10$ GeV	22.00	8.20	0.00	60.00	0.04	0.06	0.30	0.00
				60.00	0.04	0.06	0.30	0.00
				1.00	0.00	0.00	0.00	0.00
sig2+ $ m_{\tau\tau} - m_{h_1} \leq 10$ GeV	0.10	0.00	0.00	0.00	0.00	0.00	0.00	0.00
sig2+ $ m_{\tau\tau} - m_{h_2} \leq 10$ GeV	52.00	33.00	0.20	101.00	0.04	0.10	17.00	0.06
				103.00	0.04	0.10	17.00	0.06
				1.00	0.00	0.00	0.00	0.00
sig2+ $ m_{\tau\tau} - m_{h_3} \leq 10$ GeV	4.00	3.00	0.10	105.00	0.01	0.07	0.30	0.06
				104.00	0.03	0.07	0.20	0.00
				1.00	0.00	0.00	0.00	0.00

Table 7: Number of events after the selection cuts for sig2 final states for the benchmark points and backgrounds at an integrated luminosity of 10 fb^{-1} at the LHC with $E_{cm} = 14$ TeV. The different rows of background events for a given column correspond to BP1, BP2 and BP3, respectively as they differ depending on the window cuts around the mass peaks.

of luminosity but for other benchmark points one needs higher luminosity. Specially to determine the Higgs mass peak for BP3 a very high luminosity is needed.

Next we also investigated the 4ℓ final state where both the Higgses decay into lepton pairs. The prospect for this final state does not look promising at least for low luminosity and with 14 TeV LHC.

So far we have presented the dominant Standard Model (SM) backgrounds that contribute to the final states. There are other reducible model backgrounds which we also have calculated. They are $H^\pm W^\mp$, $H^\pm h_{i=1,2,3}$, $H^\pm H^\mp$, respectively. We find that their contributions are negligible for the final states we have considered here. The susy backgrounds and supersymmetric backgrounds associated with charged Higgs production have been addressed in great detail in [25] and it is shown that most of the time the final states in supersymmetric cascade decays come with large number of jets, which is unlike the case here.

5. Summary and discussion

From our analysis it is clear that the Higgs pair production is interesting in spite of being

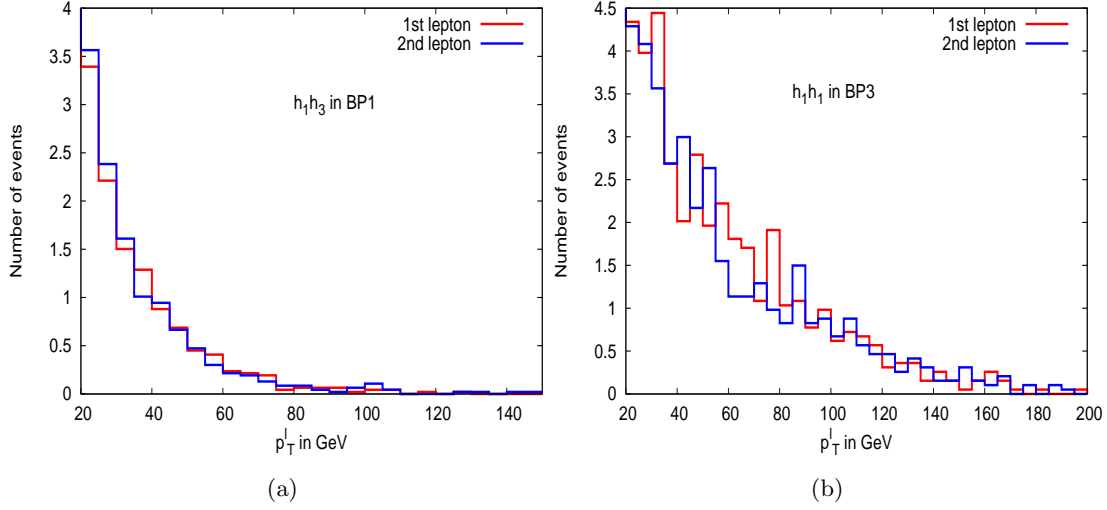


Figure 6: p_T^ℓ distribution from (a) h_1h_3 for BP1 and from (b) h_1h_1 for BP3.

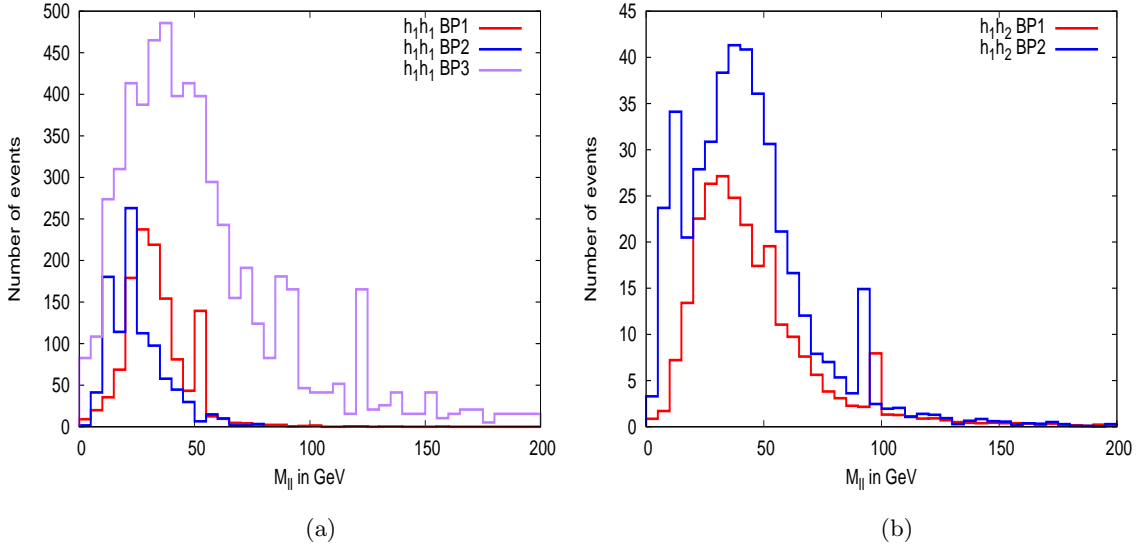


Figure 7: Lepton invariant mass distribution coming (a) from h_1h_1 , (b) from h_1h_2 for benchmark points at an integrated luminosity of $\mathcal{L} = 10 \text{ fb}^{-1}$.

electroweak production process. We have studied various possible final states that could come from the two Higgs productions. For some signal topologies an integrated luminosity of 10 fb^{-1} is enough to reach 5σ of signal significance. Specially $2b + 2\tau$ (Sig2) final state looks promising. We have seen that it is also possible to reconstruct the Higgs mass peak, both via bb invariant mass and through $\tau\tau$ invariant mass distribution.

We have also studied the leptonic final state which also has a great prospect due to its precision measurement possibility and can come handy for light Higgs mass discovery. The signal topologies coming from Higgs pair productions are very different from CP-conserving

Signal	Benchmark Points			Backgrounds				
	BP1	BP2	BP3	$t\bar{t}$	$t\bar{t}Z$	$t\bar{t}W$	VV	$t\bar{t}b\bar{b}$
sig3: 2ℓ	200.00	370.00	15.00	2007.00	52.00	43.00	1590.50	3.00
sig3+ $ m_{\ell\ell} - m_{h_1} \leq 10$ GeV	20.00	205.00	0.60	485.00	6.00	7.80	28.00	0.40
				491.00	4.00	5.00	15.00	0.70
				53.00	3.60	4.20	5.00	0.10
sig3+ $ m_{\ell\ell} - m_{h_2} \leq 10$ GeV	5.00	5.20	0.00	153.00	5.00	6.40	706.00	0.20
				156.00	5.00	6.40	710.00	0.20
				0.00	0.01	0.05	1.20	0.00
sig3+ $ m_{\ell\ell} - m_{h_3} \leq 10$ GeV	0.70	0.50	0.00	53.00	3.60	4.30	63.00	0.20
				53.00	3.60	4.30	62.00	0.20
				0.00	0.01	0.03	1.10	0.00

Table 8: Number of events after the selection cuts for 2ℓ (sig3) final states for the benchmark points and backgrounds at an integrated luminosity of 10 fb^{-1} at the LHC with $E_{cm} = 14 \text{ TeV}$. The different rows of background events for a given column correspond to BP1, BP2 and BP3, respectively as they differ depending on the window cuts around the mass peaks.

case due to the existence of the light buried Higgs. LHC at 14 TeV has a good chance to explore this possibility once it starts taking data. With more data coming in one can look for $bb\tau\tau$ or $bb\ell\ell$ invariant mass which can determine the heavy Higgs ($h_{2,3}$) mass peak and also one can distinguish $h_i Z$ events from $h_i h_j$ events.

Acknowledgments:

The authors acknowledge support from the Academy of Finland (Project No 137960). PB wants to thank Helsinki Institute of Physics for the visit during the early stages of the project and KIAS overseas travel grant. PB also thanks Prof. Jae Sik Lee for useful discussions.

References

- [1] A. Pilaftsis, Phys. Lett. B **435**, 88 (1998) [arXiv:hep-ph/9805373].
- [2] A. Pilaftsis and C. E. M. Wagner, Nucl. Phys. B **553**, 3 (1999) [arXiv:hep-ph/9902371];
- [3] D. A. Demir, Phys. Rev. D **60**, 055006 (1999) [arXiv:hep-ph/9901389];
- [4] S. Y. Choi, M. Drees and J. S. Lee, Phys. Lett. B **481**, 57 (2000) [arXiv:hep-ph/0002287];
- [5] M. S. Carena, J. R. Ellis, A. Pilaftsis and C. E. M. Wagner, Nucl. Phys. B **586** (2000) 92 [hep-ph/0003180].
- [6] G. L. Kane and L. T. Wang, Phys. Lett. B **488**, 383 (2000) [arXiv:hep-ph/0003198];
- [7] M. Dugan, B. Grinstein and L. J. Hall, Nucl. Phys. B **255** (1985) 413. S. Dimopoulos and S. D. Thomas, Nucl. Phys. B **465** (1996) 23 [arXiv:hep-ph/9510220]. Y. Kizukuri, N. Oshimo, Phys. Rev. D **46**, 3025-3033 (1992).

- [8] P. Nath, Phys. Rev. Lett. **66**, 2565 (1991); Y. Kizukuri and N. Oshimo, Phys. Rev. D **46**, 3025 (1992); T. Ibrahim and P. Nath Phys. Lett. B **418**, 98 (1998); Phys. Rev. D **57**, 478 (1998); *ibid* D **58**, 019901(E) (1998); *ibid* D **60**, 079903 (1999); *ibid* D **60**, 119901 (1999); M. Brhlik, G.J. Good and G.L. Kane, Phys. Rev. D **59**, 115004 (1999); A. Bartl, T. Gajdosik, W. Porod, P. Stockinger and H. Stremnitzer, Phys. Rev. D **60**, 073003 (1999); D. Chang, W.-Y. Keung and A. Pilaftsis, Phys. Rev. Lett. **82**, 900 (1999); S. Pokorski, J. Rosiek and C.A. Savoy, Nucl. Phys. B **570**, 81 (2000); E. Accomando, R. Arnowitt and B. Dutta, Phys. Rev. D **61**, 115003 (2000); S. Abel, S. Khalil and O. Lebedev, Nucl. Phys. B **606**, 151 (2001); U. Chattopadhyay, T. Ibrahim and D.P. Roy, Phys. Rev. D **64**, 013004 (2001); D.A. Demir, M. Pospelov and A. Ritz, hep-ph/0208257.
- [9] A. Pilaftsis, Nucl. Phys. B **644**, 263 (2002).
- [10] T. Falk, K.A. Olive, M. Pospelov and R. Roiban, Nucl. Phys. B **60**, 3 (1999).
- [11] S. Chatrchyan *et al.* [CMS Collaboration], Phys. Lett. B **716** (2012) 30 [arXiv:1207.7235 [hep-ex]].
- [12] G. Aad *et al.* [ATLAS Collaboration], Phys. Lett. B **716** (2012) 1 [arXiv:1207.7214 [hep-ex]].
- [13] CMS-PAS-HIG-13-001
- [14] ATLAS-CONF-2013-012
- [15] R. Barate *et al.* [LEP Working Group for Higgs boson searches], Phys. Lett. B **565**, 61 (2003) [arXiv:hep-ex/0306033];
see also [http : //lephiggs.web.cern.ch/LEPHIGGS/www/Welcome.html](http://lephiggs.web.cern.ch/LEPHIGGS/www/Welcome.html)
- [16] S. Schael *et al.* [ALEPH Collaboration], Eur. Phys. J. C **47**, 547 (2006) [arXiv:hep-ex/0602042];
see also [http : //lephiggs.web.cern.ch/LEPHIGGS/www/Welcome.html](http://lephiggs.web.cern.ch/LEPHIGGS/www/Welcome.html)
G. Abbiendi *et al.* [OPAL Collaboration], Eur. Phys. J. C **37** (2004) 49 [hep-ex/0406057].
- [17] [Tevatron New Physics Higgs Working Group and CDF and D0 Collaborations], arXiv:1207.0449 [hep-ex].
- [18] See: LEP Higgs Working Group, LHWG-Note 2004-01.
- [19] P. Bechtle [LEP Collaboration], PoS **HEP2005**, 325 (2006) [arXiv:hep-ex/0602046].
- [20] M. S. Carena, J. R. Ellis, A. Pilaftsis and C. E. M. Wagner, Phys. Lett. B **495**, 155 (2000) [arXiv:hep-ph/0009212].
- [21] A. Pilaftsis, Phys. Rev. D **58**, 096010 (1998) [arXiv:hep-ph/9803297].
- [22] M. S. Carena, J. R. Ellis, S. Mrenna, A. Pilaftsis and C. E. M. Wagner, Nucl. Phys. B **659**, 145 (2003) [arXiv:hep-ph/0211467].
- [23] S. P. Das, M. Drees,
[arXiv:1010.3701 [hep-ph]]. S. P. Das, M. Drees,
[arXiv:1010.2129 [hep-ph]].
- [24] E. Accomando *et al.*, [arXiv:hep-ph/0608079].
- [25] P. Bandyopadhyay,
[arXiv:1008.3339 [hep-ph]].
- [26] Z. Li, C. S. Li and Q. Li, Phys. Rev. D **73**, 077701 (2006) [arXiv:hep-ph/0601148];

- [27] P. Bandyopadhyay, A. Datta, A. Datta *et al.*, Phys. Rev. **D78** (2008) 015017. [arXiv:0710.3016 [hep-ph]].
- [28] P. Bandyopadhyay, JHEP **0907** (2009) 102. [arXiv:0811.2537 [hep-ph]]; P. Bandyopadhyay, A. Datta, B. Mukhopadhyaya, Phys. Lett. **B670** (2008) 5-11. [arXiv:0806.2367 [hep-ph]]; K. Huitu, R. Kinnunen, J. Laamanen *et al.*, Eur. Phys. J. **C58** (2008) 591-608. [arXiv:0808.3094 [hep-ph]]; A. Datta, A. Djouadi, M. Guchait *et al.*, Nucl. Phys. **B681** (2004) 31-64. [hep-ph/0303095]; A. Datta, A. Djouadi, M. Guchait *et al.*, Phys. Rev. **D65** (2002) 015007. [hep-ph/0107271]; G. D. Kribs, A. Martin, T. S. Roy and M. Spannowsky, arXiv:1006.1656 [hep-ph]; G. D. Kribs, A. Martin, T. S. Roy and M. Spannowsky, Phys. Rev. **D 81** (2010) 111501 [arXiv:0912.4731 [hep-ph]].
- [29] D. K. Ghosh, S. Moretti, Eur. Phys. J. **C42** (2005) 341-347 [hep-ph/0412365]; D. K. Ghosh, R. M. Godbole, D. P. Roy, Phys. Lett. **B628** (2005) 131-140 [hep-ph/0412193]; S. Y. Choi, K. Hagiwara and J. S. Lee, Phys. Rev. D **64**, 032004 (2001) [arXiv:hep-ph/0103294]; S. Y. Choi, K. Hagiwara and J. S. Lee, Phys. Lett. B **529**, 212 (2002) [arXiv:hep-ph/0110138]; S. Heinemeyer, Eur. Phys. J. C **22**, 521 (2001) [arXiv:hep-ph/0108059]; T. Ibrahim and P. Nath, Phys. Rev. D **66**, 015005 (2002) [arXiv:hep-ph/0204092]; S. W. Ham, S. K. Oh, E. J. Yoo, C. M. Kim and D. Son, Phys. Rev. D **68**, 055003 (2003) [arXiv:hep-ph/0205244]. J. S. Lee, AIP Conf. Proc. **1078** (2009) 36 [arXiv:0808.2014 [hep-ph]].
- [30] R. Barate *et al.* [LEP Working Group for Higgs boson searches and ALEPH Collaboration and and], Phys. Lett. B **565**, 61 (2003) [arXiv:hep-ex/0306033]. G. Abbiendi *et al.* [OPAL Collaboration], Eur. Phys. J. C **37** (2004) 49 [hep-ex/0406057].
- [31] J. R. Ellis, J. S. Lee and A. Pilaftsis, JHEP **0810** (2008) 049 [arXiv:0808.1819 [hep-ph]].
- [32] K. Cheung, O. C. W. Kong and J. S. Lee, JHEP **0906** (2009) 020 [arXiv:0904.4352 [hep-ph]]. J. Ellis, J. S. Lee and A. Pilaftsis, JHEP **1102** (2011) 045 [arXiv:1101.3529 [hep-ph]].
- [33] B. C. Regan, E. D. Commins, C. J. Schmidt and D. DeMille, Phys. Rev. Lett. **88** (2002) 071805.
- [34] P. Franzini, D. Son, P. M. Tuts, S. Youssef, T. Zhao, J. Lee-Franzini, J. Horstkotte and C. Klopfenstein *et al.*, Phys. Rev. D **35** (1987) 2883. J. S. Lee and S. Scopel, Phys. Rev. D **75** (2007) 075001 [hep-ph/0701221 [HEP-PH]].
- [35] S. Chatrchyan *et al.* [CMS Collaboration], arXiv:1307.5025 [hep-ex]. RAaij *et al.* [LHCb Collaboration], arXiv:1307.5024 [hep-ex]. RAaij *et al.* [LHCb Collaboration], Phys. Rev. Lett. **110** (2013) 021801 [arXiv:1211.2674 [hep-ex]].
- [36] S. L. Glashow, J. Iliopoulos and L. Maiani, Phys. Rev. D **2** (1970) 1285.
- [37] S. Chatrchyan *et al.* [CMS Collaboration], arXiv:1303.2985 [hep-ex]. ATLAS-CONF-2013-047
- [38] Y. Amhis *et al.* [Heavy Flavor Averaging Group Collaboration], arXiv:1207.1158 [hep-ex].
- [39] M. S. Carena, D. Garcia, U. Nierste and C. E. M. Wagner, Phys. Lett. B **499** (2001) 141 [hep-ph/0010003]. G. Degrandi, P. Gambino and G. F. Giudice, JHEP **0012** (2000) 009 [hep-ph/0009337].
- [40] G. Aad *et al.* [ATLAS Collaboration], arXiv:1308.2631 [hep-ex]. G. Aad *et al.* [ATLAS Collaboration], arXiv:1308.1841 [hep-ex]. S. Chatrchyan *et al.* [The CMS Collaboration], arXiv:1308.1586 [hep-ex]. See also
'http://moriond.in2p3.fr/QCD/2013/MondayMorning/Favareto.pdf'

- [41] ATLAS-CONF-2013-007, CMS-PAS-SUS-13-007
- [42] J. S. Lee, M. Carena, J. Ellis, A. Pilaftsis and C. E. M. Wagner, *Comput. Phys. Commun.* **184** (2013) 1220 [arXiv:1208.2212 [hep-ph]].
 J. S. Lee, M. Carena, J. Ellis, A. Pilaftsis and C. E. M. Wagner, *Comput. Phys. Commun.* **180** (2009) 312 [arXiv:0712.2360 [hep-ph]].
 J. S. Lee, A. Pilaftsis, M. S. Carena, S. Y. Choi, M. Drees, J. R. Ellis and C. E. M. Wagner, *Comput. Phys. Commun.* **156**, 283 (2004) [arXiv:hep-ph/0307377]. J. R. Ellis, J. S. Lee and A. Pilaftsis, *Mod. Phys. Lett. A* **21**, 1405 (2006) [arXiv:hep-ph/0605288].
 See also 'http://www.hep.man.ac.uk/u/jslee/dist/CPsuperH/v2/tables.2010.Jun.pdf'
- [43] T. Hahn, S. Heinemeyer, W. Hollik, H. Rzehak, G. Weiglein and K. Williams, [arXiv:hep-ph/0611373].
- [44] [Tevatron Electroweak Working Group and CDF and D0 Collaborations], arXiv:1107.5255 [hep-ex].
- [45] A. Pukhov, "CalcHEP 3.2: MSSM, structure functions, event generation, batchs, and generation of matrix elements for other packages", [arXiv:hep-ph/0412191].
- [46] See "http://www.personal.soton.ac.uk/ab1u06//public/calchep/"
- [47] P. Skands *et al.*, *JHEP* **0407**, 036 (2004) [arXiv:hep-ph/0311123];
 see also <http://home.fnal.gov/~skands/slha/>
- [48] T. Sjostrand, L. Lonnblad and S. Mrenna, [arXiv:hep-ph/0108264].
- [49] H. L. Lai *et al.* [CTEQ Collaboration], *Eur. Phys. J. C* **12**, 375 (2000) [arXiv:hep-ph/9903282].
- [50] J. Pumplin, D. R. Stump, J. Huston, H. L. Lai, P. Nadolsky and W. K. Tung, *JHEP* **0207**, 012 (2002) [arXiv:hep-ph/0201195].
- [51] M. Cacciari, G. P. Salam and G. Soyez, *Eur. Phys. J. C* **72** (2012) 1896 [arXiv:1111.6097 [hep-ph]].
- [52] http://www-d0.fnal.gov/flera/btag_note4432.pdf
 I Tomalin, 2008 J. Phys.: Conf. Ser. 110 092033
 H. Baer, V. Barger, G. Shaughnessy, H. Summy and L. t. Wang, *Phys. Rev. D* **75**, 095010 (2007) [arXiv:hep-ph/0703289].
- [53] G. L. Bayatian *et al.* [CMS Collaboration], *J. Phys. G* **G34** (2007) 995-1579.
- [54] G. Bagliesi, [arXiv:0707.0928 [hep-ex]].